AD-A033 124 TRACOR INC AUSTIN TEX F/G 17/1

THE DISTORTION OF A SONAR PULSE REFLECTED FROM THE OCEAN SURFAC--ETC(U)

MAR 68 H P BUCKER, G I BOURIANOFF N00024-67-C-1318

UNCLASSIFIED TRACOR-68-343-U NL

1 OF 1
AD
A033124

END

DATE
FILMED
2-77

Contract N00024-67-C-1318
Project Serial SF101-03-16
Task 8524
TRACOR Project 002 046 01
Document Number 68-343-U

TECHNICAL MEMORANDUM

THE DISTORTION OF A SONAR PULSE REFLECTED FROM THE OCEAN SURFACE

by

H. P. Bucker G. I. Bourianoff

Submitted to:

Commander, Naval Ship Systems Command
Department of the Navy
Washington, D. C. 20360

Attn: Code 00V1C

March 1, 1968

TRACOR

6500 Tracor Lane, Austin, Texas 78721, AC 512/926-2800

TRACOR 6500 TRACOR LANE, AUSTIN, TEXAS 78721

(15) Contract N00024-67-C-1318
Project Serial SF101-03-16
Task 8524
TRACOR Project 002 046 01
Document Number 68-343-U

(14) TRACOR-68-343-U

(16) F10103

(17) SF1010316

(9) TECHNICAL MEMORANDUM

(6) THE DISTORTION OF A SONAR PULSE REFLECTED FROM THE OCEAN SURFACE

by

(10) H. P. Bucker G. I. Bourianoff

Submitted to:

Commander, Naval Ship Systems Command
Department of the Navy
Washington, D. C. 20360

Attn: Code 00V1C

March 1, 1968

(11) 1 Mar 68

(12) 47p.

Approved:

W. C. Moyer
W. C. Moyer
Program Manager

Submitted:

H. P. Bucker
H. P. Bucker
Project Director

352 100
6pg

680308-0071

ABSTRACT

Equations are derived for the direct evaluation of a sonar pulse reflected from a time-varying ocean surface. Fewer assumptions and approximations are made in this direct approach than in conventional developments of scattering theory. However, the cost of computer time may become excessive for some cases.

The calculated surface reflected signals are correlated with the incident sonar pulse to find the expected correlation loss of a sonar processor. For a short (5 msec) low frequency FM slide the calculated correlation losses (1.6 dB for the surface generated by a 10 knot wind and 3.9 dB for a 20 knot wind) were almost entirely the result of energy loss in the reflected signal.

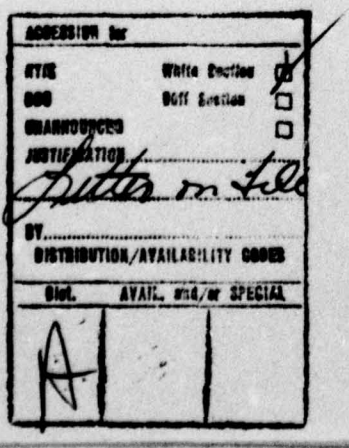

TABLE OF CONTENTS

LIST OF ILLUSTRATIONS

1. INTRODUCTION

In most operations, an active sonar system must process a signal which has reflected, in part or whole, from the ocean surface. The effect of signal distortion because of the surface reflection should be understood if the processing system is to do a good job of identifying possible target echoes.

Many investigators[1-5] have made experimental measurements of backscattering coefficients. Forward scattering coefficients are more difficult to measure because the source and receiver must be separated. Measurements have been reported by Liebermann[6] and Marsh[4].

Many theoretical studies have been reported where equations are derived relating the scattering coefficient to sea state parameters for a stationary surface[7-12]. All of these theories assume the incident wave to be single frequency, continuous, and plane. Also, all of these theories contain approximations that become invalid as the surfaces become rough or the grazing angles become small. As would be expected, the theoretical predictions are accurate for large grazing angles and reasonably smooth surfaces but have limited usefulness under other conditions.

Model scattering experiments have been reported by La Casce and Tamarkin[13], by Horton, Mitchell, and Barnard[14], and by Medwin[15]. These have been most helpful in testing the different theoretical approaches to the scattering problem. Their usefulness in helping to understand the active sonar problems has been limited, however, because of the difficulty in scaling the model results to the full size ocean environment.

The reflection of a sinusoidal wave from a time varying surface has been studied by Liebermann[16], Marsh[17] and Parkins[18]. Liebermann demonstrated the presence of Doppler shifted components

in the reflected signal. Marsh made modifications to his earlier work so that the Doppler shifts could be calculated. Parkins developed the theory in such a manner that explicit forms of the spectral density of the reflected waves were obtained in the limiting cases of slightly rough and very rough surfaces.

The above references are only a small fraction of the papers concerning scattering theory. They were listed because they represent significant advances in the field and because they indicate the current points of attack on the problem. However, in none of the above references, or in any other literature reviewed, is any method for accurately calculating the distortion of a sonar pulse when it reflects from this time varying ocean surface. To answer this question, work was begun at TRACOR to develop a direct calculation of the reflected sonar pulse using Kirchoff's integral. Details of the calculation are given in Section 4.

Although the assumptions usually made in scattering theory were not required in the equations developed here, the present method is limited by its running time on a computer. The running time is proportional to the number of reflecting areas on the surface and to the length of the pulse. In order to study long pulses (a 500 msec 3.5 kHz pulse contains over 1700 cycles), the surface insonification has been limited in the present work to a strip one meter wide with the strip length determined by the 3 dB down points of the beam pattern. It seems plausible that this narrow beam will have about the same distortion as a more typical sonar beam, but this supposition remains to be proved.

Section 3 describes the generation of the ocean surface. The surface is formed by a set of 100 moving cosinusoidal waves with random phases. Choosing a new set of phases will result in a completely different surface, but one that has the

same energy spectrum. Thus the two surfaces are different samples from the same sea.

In Sections 5 and 6 some typical reflected signals are displayed and the distortion in the reflected pulse is determined by means of replica correlation. Correlation losses that would occur in typical sonar processors are calculated.

Section 7 describes an attempt to improve the operation of a correlator by modifying the replica to fit the distortion in the reflected signal. Although the improvement gained in the correlator output was nil, this result has significance.

Section 8 describes a simple method of setting a general type of pulse (such as a pseudo random noise pulse) in a form suitable for efficient evaluation of Kirchoff's integral.

2. SUMMARY

Equations have been derived and a computer program written for the calculation of a sonar pulse that reflects from the time-varying ocean surface. No restrictions on the size of the waves or type of sonar pulse are inherent in the program, although the cost of computer time may become excessive for some cases.

To calculate the sonar distortion for a typical ping, the pulse form, beam shape, and wind speed are specified. The program then generates a time varying sample of the ocean surface and the reflected pulse is calculated by a direct evaluation of Kirchoff's integral. The program can be run again with the same input parameters but with a different sample of the surface. Thus, ping to ping variation of the reflected pulses can be studied in a quantitative manner.

The effect of the surface reflection is separated into two parts. First, the fluctuation of energy in the reflected pulse for successive pings, i.e., for different surface realizations, is tabulated. Second, the amount of correlation loss because of signal distortion is calculated by comparing the correlator output for the reflected signal with the correlator output for the pulse reflected from a flat surface. For a short, 5 msec, FM slide the correlation loss for a 10 knot wind speed was 1.6 dB, all of which was due to energy loss. The correlation loss for a 20 knot wind speed was 3.9 dB, of which 3.8 dB was due to energy loss.

Equations are developed for matching the correlator replica to the distorted pulse, however, the correlator improvement was negligible. Finally, a generalization is discussed that will permit calculation of reflected pseudo random noise pulses and reflected explosive pulses.

3. SIMULATION OF THE SEA SURFACE

The moving sea surface is simulated by superimposing a large number of cosinusoidal waves of random phase. This model is called a long-crested Gaussian linear Eulerian model of random waves[19]. The elevation of the sea surface, z, as a function of distance, in the direction the waves are traveling, and time is

$$z(x,t) = \sum_{n=1} a_{2n+1} \cos(k_{2n+1}x - \omega_{2n+1}t + \epsilon_{2n+1}) \ .$$

For deep water k is equal to ω^2/g, ω is the angular frequency, g is the gravitational constant, and the $\{\epsilon\}$ are a set of random phases chosen from a distribution uniform over 0 to 2π. The coefficients of the traveling cosine waves, a, are related to the spectral density of the sea surface $S(\omega)$ by[19]

$$a_{2n+1} = [2S(\omega_{2n+1}) \cdot (\omega_{2n+2} - \omega_{2n})]^{\frac{1}{2}} \ .$$

Using semi-empirical arguments as to the form of $S(\omega)$ and a large number of experimental data points Pierson and Moskowitz[20] derived the following formula for $S(\omega)$:

$$S(\omega) = (\alpha g^2/\omega^5) \exp(-\beta(g/(v\omega))^4) \ .$$

Here ω is the angular frequency, g is 9.8 m/sec^2, v is the wind velocity in m/sec, and α and β are dimensionless constants with $\alpha = 0.0081$ and $\beta = 0.74$. Figure 3-1 is a plot of $S(\omega)$ vs frequency for some typical values of wind speed in knots.

Samples of the sea surface at different times are generated by superimposing 100 traveling cosine waves with random phases shown in Figs. 3-2, -3, -4, -5. Figures 3-2, 3-3, and 3-5 were calculated using the same set of random phases but correspond to wind speeds of 5, 10, and 20 knots respectively. The

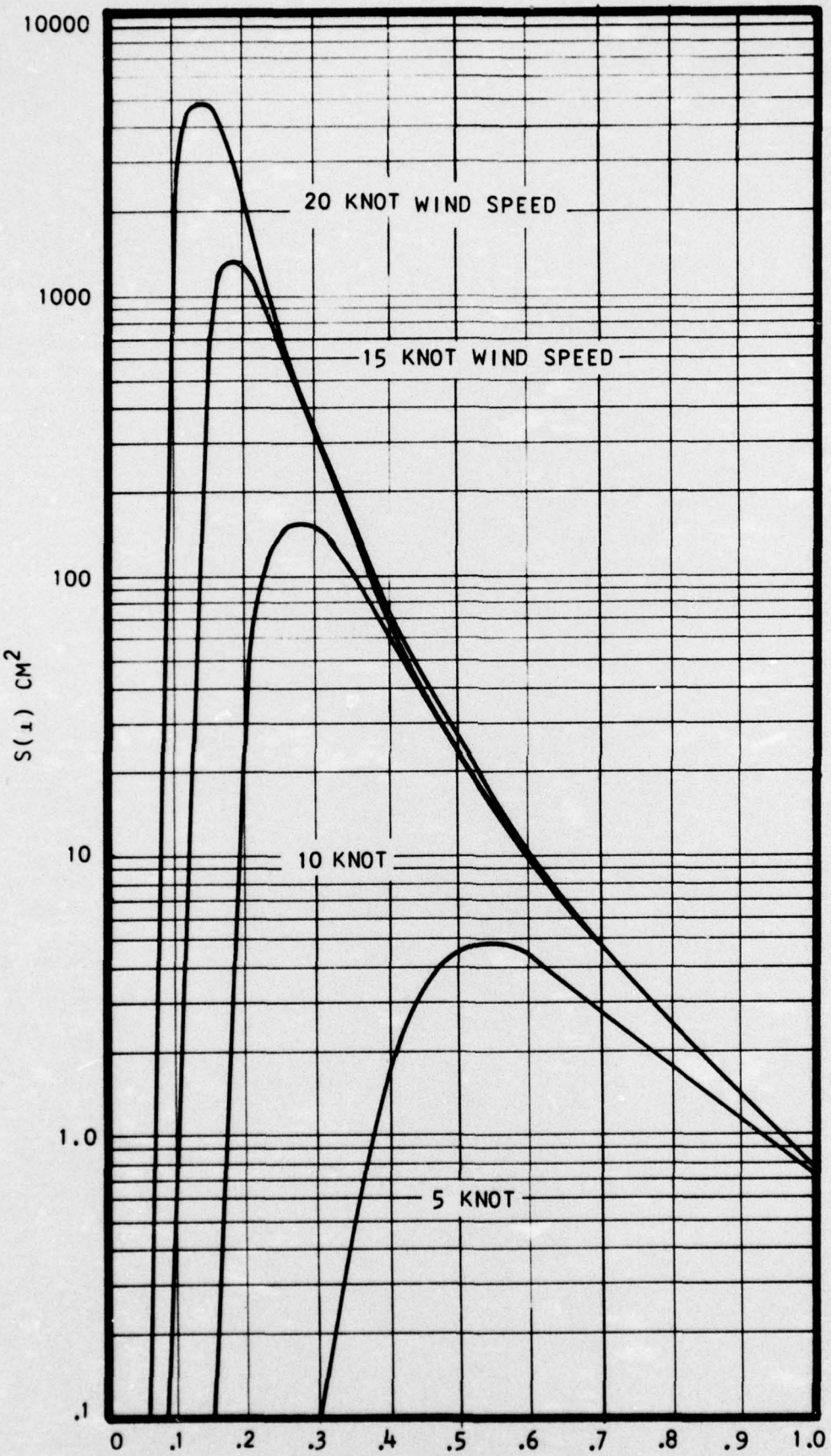

FIG. 3-1 - WAVE SPECTRUM S(ω) VS FREQUENCY FOR OCEAN WAVES

TRACOR, INC A6-140-1
AUSTIN, TEXAS 12/14/67 BUCKER01

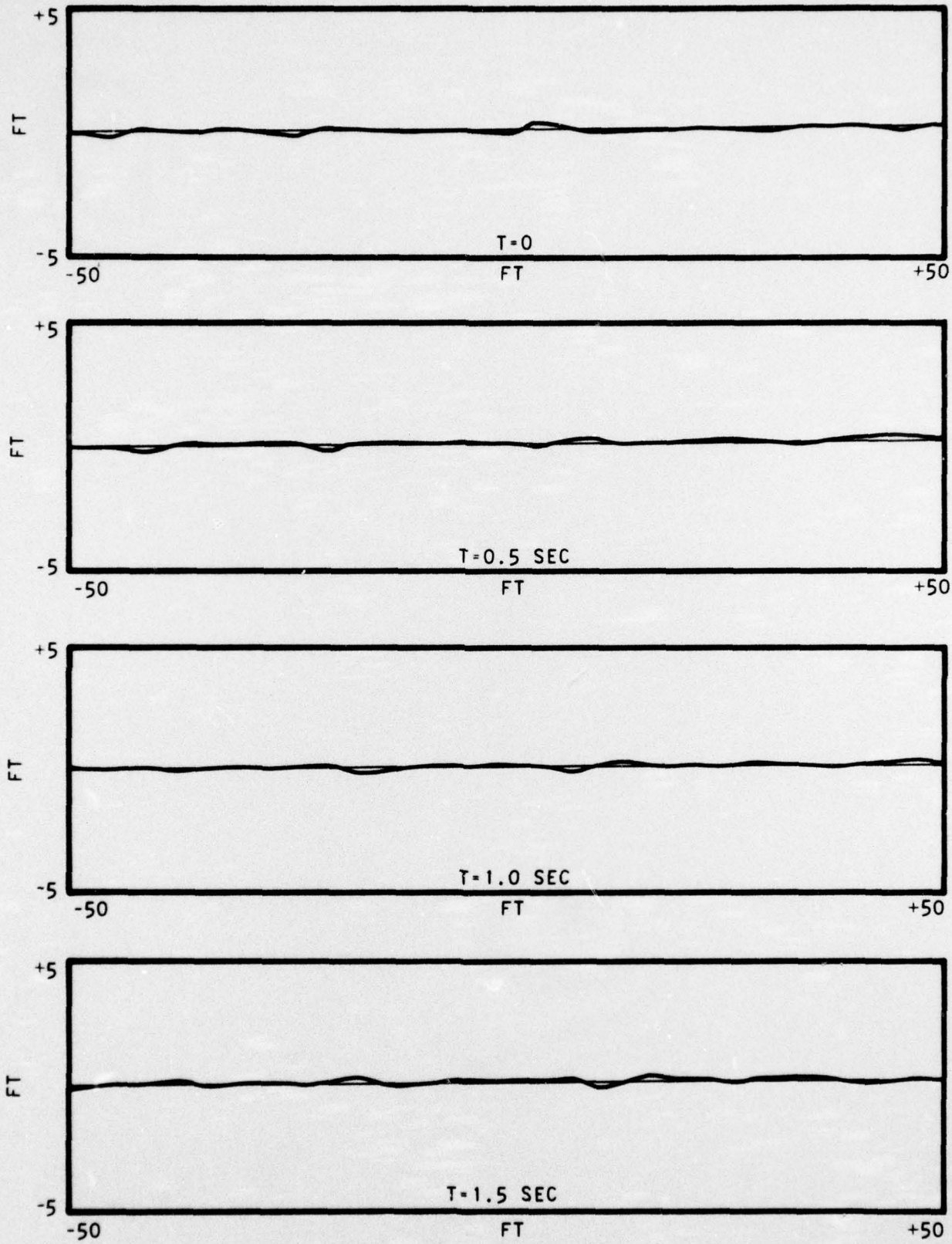

FIG. 3-2 - NEUMANN-PIERSON MODEL OF THE SEA SURFACE AT FOUR TIMES FOR A 5 KNOT WINDSPEED

TRACOR DWG. A6-104-6
2/8/68 BOURIANOFF

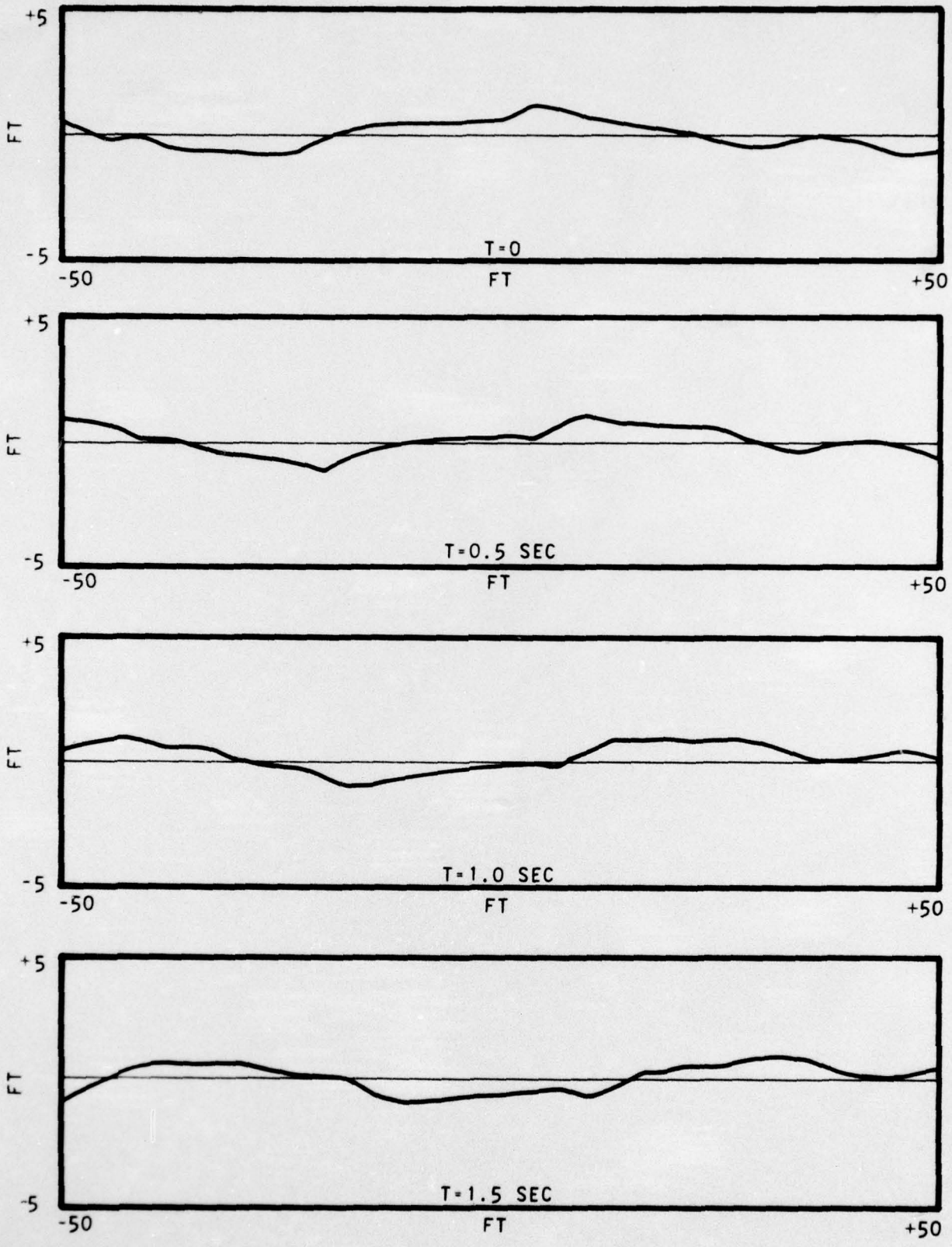

FIG. 3-3 - NEUMANN-PIERSON MODEL OF THE SEA SURFACE AT FOUR TIMES FOR A 10 KNOT WINDSPEED

TRACOR DWG. A6-104-4
2/8/67 BOURIANOFF

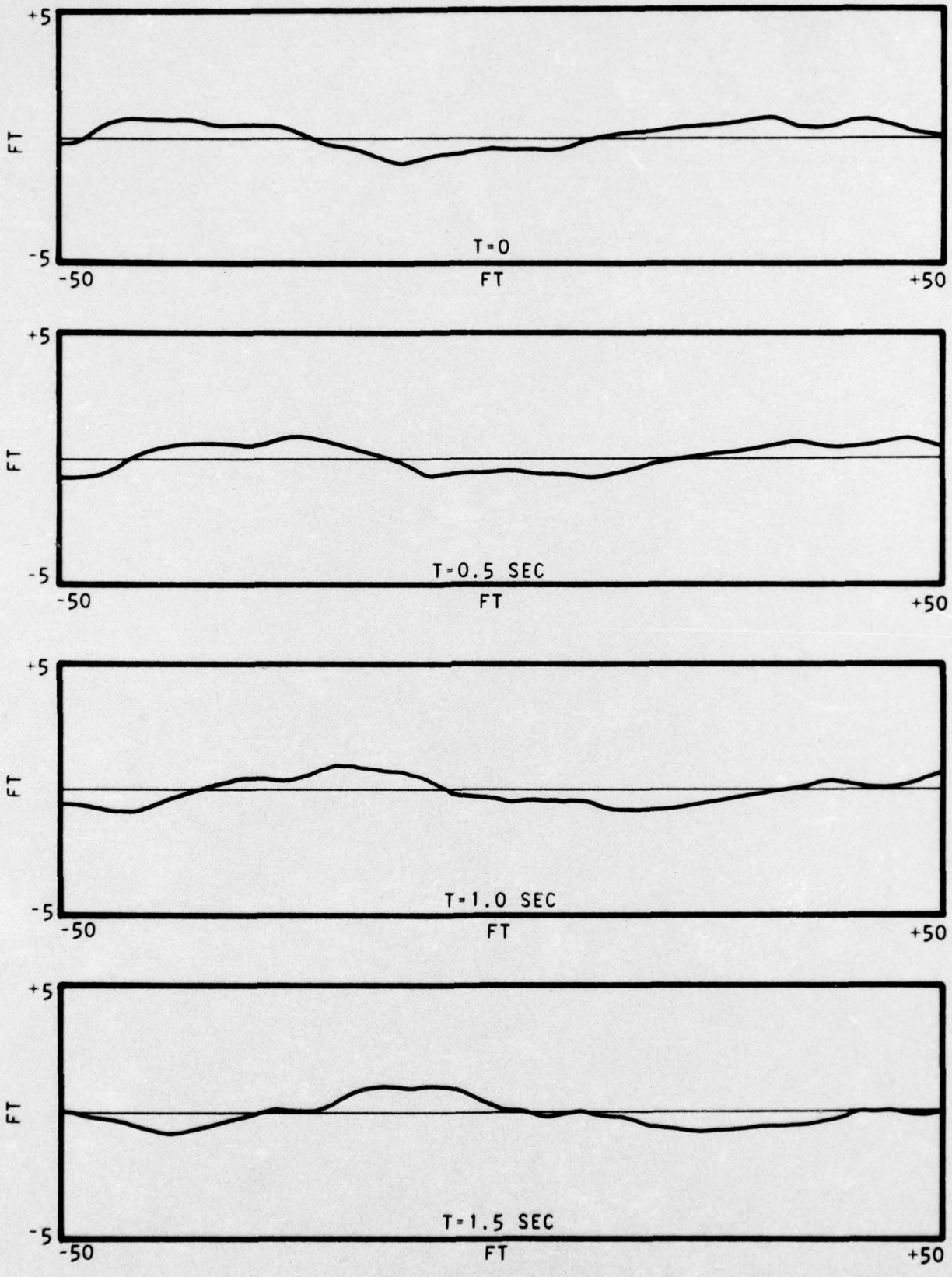

FIG. 3-4 - ANOTHER REALIZATION OF THE SEA SURFACE FOR A 10 KNOT WINDSPEED

TRACOR DWG A6-140-7
2/8/68 BOURIANOFF

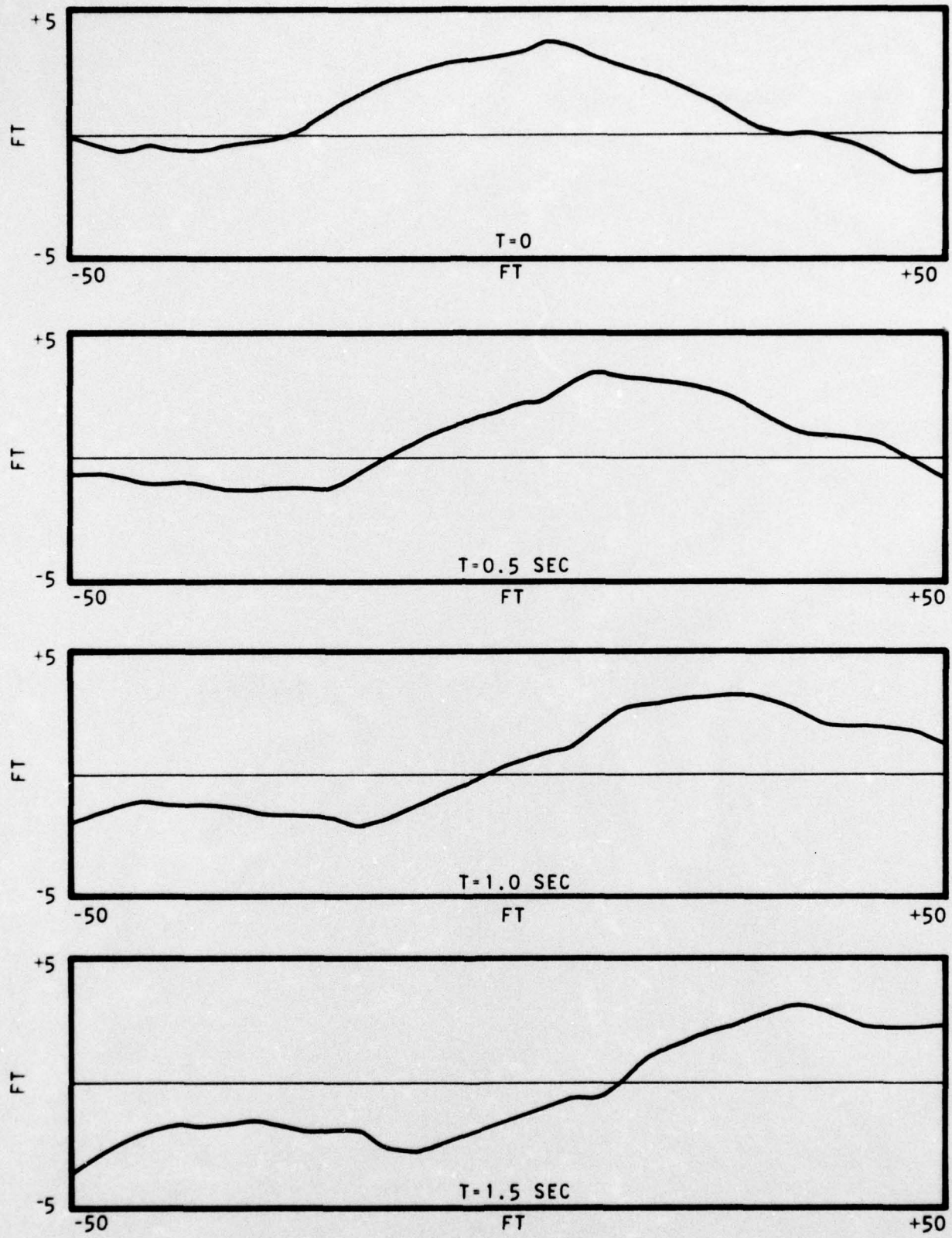

FIG. 3-5 - NEUMANN-PIERSON MODEL OF THE SEA SURFACE AT FOUR TIMES FOR A 20 KNOT WINDSPEED

TRACOR DWG. A6-104-5
2/8/68 BOURIANOFF

four curves in each of the figures represent the surface at four consecutive times separated by ½ sec intervals. Figure 3-4 corresponds to a 10 knot wind speed but for a different set of random phases. Thus Figs. 3-3 and 3-4 correspond to different samples, or representations, of the same sea.

4. MATHEMATICAL FORM OF THE REFLECTED PULSE

In this section an equation is derived for calculation of the reflected pulse as a function of the incident pulse form, the geometry of the problem, and the motion of the surface. Referring to Fig. 4-1, the source at x_s, z_s emits a pulse described in terms of a velocity potential $f(t)D(\theta)$. The pulse form is determined by $f(t)$ while $D(\theta)$ takes care of the beam pattern and level of the source. The equation of the moving surface is $z = z(x,t)$.

Consider the problem if the surface were removed. The potential at any point p would be

$$\Phi = f(ct - \rho) \cdot D(\theta)/\rho \ , \qquad (4.1)$$

where ρ is the distance from the source to p and c is the velocity of sound. With the surface in place the potential at p, any point in the water or at the surface can be written as $f(t - \rho/c) \cdot D(\theta)/\rho + U$. Because U is a potential due to the presence of the surface it may be called the scattered potential function. Since the acoustical pressure must be zero at the surface,

$$f(ct - \rho) \cdot D(\theta)/\rho + U = 0 \text{ (at the surface)} \ . \qquad (4.2)$$

Following Eckhart[8], the normal derivative of U, $\partial U/\partial n$, is equal to plus or minus the normal derivative of the incident field depending upon whether the paths from the source and receiver to the surface point are clear or shadowed. Thus

$$\frac{\partial U}{\partial n} = q\, D(\theta)\, \frac{\partial}{\partial n}(f(ct - \rho)) \ , \qquad (4.3)$$

where q is +1 for a clear surface area and -1 for a shadowed area.

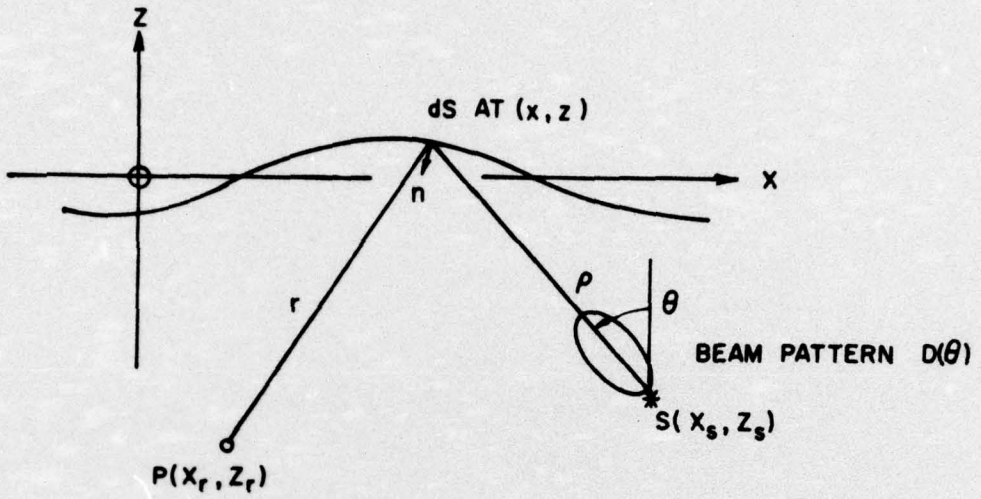

FIG. 4-1A

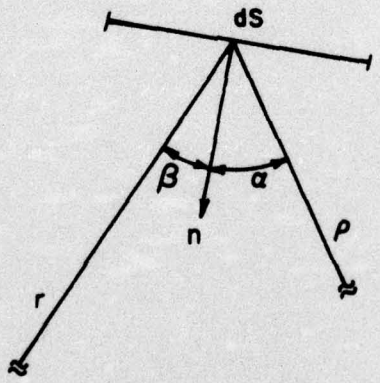

FIG. 4-1B

FIG. 4-1 - GEOMETRY OF SCATTERING SYSTEM

The complete and rigorous solution for the reflected sound field can be written in terms of the Kirchoff integral[21]

$$U_p = \frac{1}{4\pi} \iint_s \{[U_s] \frac{\partial}{\partial n}(\frac{1}{r}) - \frac{1}{cr} \frac{\partial r}{\partial n}[\frac{\partial U_s}{\partial t}] - \frac{1}{r}[\frac{\partial U_s}{\partial n}]\} \, dS. \quad (4.4)$$

Here U_p is the velocity potential of the scattered pulse at a point P, and U_s is the potential at the surface. The integral is summed over the insonified surface and the square brackets [] mean that the potential functions should be retarded. Referring to Eqs. (4.2), (4.3) and Fig. 4-1 it is not difficult to show that at the surface,

$$\begin{aligned} U_s &= - f(ct - \rho)/\rho \\ [U_s] &= - f(ct - s)/\rho \ , \ s = r + \rho \\ \partial U_s/\partial n &= q \, \partial\{f(ct - \rho)/\rho\}/\partial n \\ \partial/\partial n &\rightarrow - \cos\alpha \, \partial/\partial\rho \\ \partial U_s/\partial t &= -(1/\rho) \, \partial f(ct - \rho)/\partial t = (-c/\rho) f' \\ \partial r/\partial n &= - \cos\beta \\ \partial(1/r)/\partial r &= \cos\beta/r^2 \ . \end{aligned} \quad (4.5)$$

Substituting (4.5) into (4.4), and with some more algebraic reduction, Kirchoff's integral can be written as

$$U_p(t) = - \frac{D(\theta)}{4\pi} \iint_s \{[f](\frac{\cos\beta}{\rho r^2} + \frac{q\cos\alpha}{\rho^2 r} + [f'](\frac{\cos\beta}{\rho r} + \frac{q\cos\alpha}{\rho r})\} \, dS \ . \quad (4.6)$$

The significance of the two values of q can be made clear by using Eq. (4.6) to calculate the pulse reflected from a perfectly flat pressure release surface. It can be shown that if q is equal to one, the reflected pulse is a perfect replica of the incident pulse but with change of sign, which is the same answer as from the method of images. If q is -1 the reflected pulse is identically zero which is the appropriate return from a shadowed section of the rough surface. Finding the shadowed areas is a straight-forward problem; however, in the cases considered so far all surface elements have been assumed to be clear. An estimate of the fraction of scattered areas can be made using equations derived by Wagner[22].

Any attempt at direct evaluation of Eq. (4.6) leads to considerable difficulty. For example, for a given t the location and orientation of each surface element must be found at the earlier time at which the surface element reflected the sound energy which arrives at the receiver P at t. A much easier approach is to focus attention on a single surface element, for example, the surface between x_1 and x_2 in Fig. 4-2, and calculate the complete reflected signal from this region as a function of time. The region of interest is then shifted to an adjacent area, the reflected signal calculated and, using the principle of superposition, the second signal is weighted according to Eq. (4.6) and added to that already calculated. When all regions have been covered the complete reflected signal has been calculated. A simple example will illustrate the details of the calculation.

Consider a pulse made up of two one-cycle sine waves, with periods T_1 and T_2, as shown in Fig. 4-2*. The time when the

*In this section we will assume that f(t) can be represented by a set of sinusoidal cycles. The period of each cycle may be chosen as any function of time. This provides an excellent representation of CW pulses and FM slides. In a later section it will be shown how any reasonable form of f(t), including pseudo-random noise pulses and explosive pulses, can be built up of segments of sinusoidal waves plus a DC component. The computer time using the more general pulse will not be appreciably greater than for the pulses considered here.

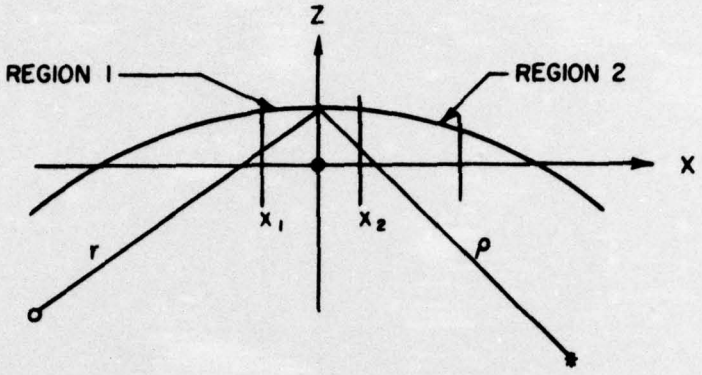

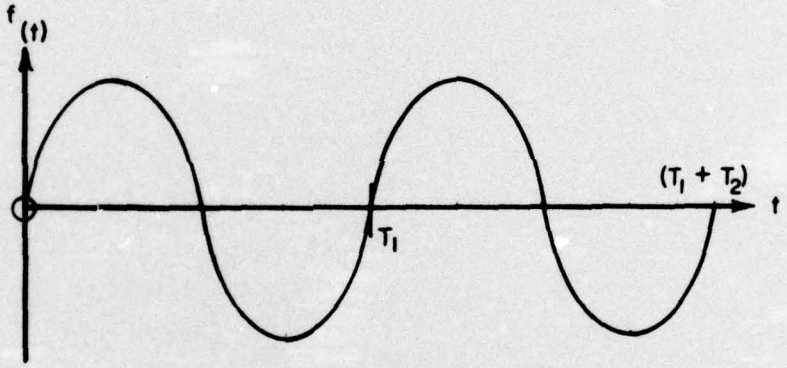

$$0 < t < T_1 \quad \begin{cases} f(ct-r) = \sin\left[k_1(ct-r)\right], & k_1 = 2\pi/(c\,T_1) \\ f'(ct-r) = k_1\cos(ct-r) \end{cases}$$

$$T_1 < t < T_2 \quad \begin{cases} f(ct-r) = \sin\left[k_2(c(t-T_1)-r)\right], & k_2 = 2\pi/(c\,T_2) \\ f'(ct-r) = k_2\cos\left[c(t-T_1)-r\right] \end{cases}$$

FIG. 4-2 - SAMPLE CASE FOR TWO CYCLE PULSE

beginning of the first cycle reflects from region 1 is found as follows. If the surface were flat, this time would be $t^o = \rho^o/c$, where ρ^o is the distance between the source and a flat surface in region 1. Let z^o be the actual surface elevation at this time and $\dot{z}^o$ be the z component of surface velocity. Then the correction to the time of reflection is $|z_s| z^o/(\rho^o c - |z_s| \dot{z}^o)$, where z_s is the z coordinate of the source. The time of arrival of the beginning of the first cycle at the receiver is $\rho^o/c + r^o/c + \delta t_1$, where r^o is the distance between the receiver and the flat surface in region 1 and

$$\delta t_1 = |z_s| z^o/(\rho^o c - |z_s| \dot{z}^o) + |z_r| z^o/(r^o c - |z_r| \dot{z}^o) \quad .$$

The same procedure is repeated to find the beginning of the second cycle (time = $\rho^o/c + r^o/c + T_1 + \delta t_2$) and the end of the second cycle. Now with the values of $\cos \alpha$, $\cos \beta$, and dS, for the times when the sound waves reflected from the surface element, the complete wave reflected from region 1 is determined. The wave is sampled and the sampled values are stored in a string of computer cells according to the sampling time. The whole procedure is repeated for the other surface regions and, using the principle of superposition, the sampled values of the signal from each new region are put in on top of previously calculated values in the computer.

5. CALCULATED SURFACE REFLECTED PULSES

The final objective of this project is to calculate the correlation loss and energy fluctuations that an active sonar will encounter because of surface reflections. However, the computer runs to date, which will be reported here, have been short, 5 msec, FM slides with frequencies around 1 kHz. The short pulse length obviously conserves computer time and the low frequency allows a visual inspection of the distortion in the reflected pulse. A sampling rate of 10 kHz is built into the program so that sonar systems operating at frequencies up to 5 kHz can be studied.

The most interesting result from the calculations to date is that the replica correlator does an excellent job of identifying the distorted signal. Although ping to ping fluctuations of energy levels in the reflected signals are large and the reflected signals show obvious distortion, the correlator output has no loss because of distortion in the reflected signal for a 10 knot wind speed and only 0.1 dB loss for a 20 knot wind.

Figure 5-1 shows the incident pulse used in this study and the pulse reflected from a flat ocean surface. The incident pulse is a Doppler invariant (i.e., the period of each cycle is a linear function of time) FM slide with 5 cycles sweeping from 950 to 1050 Hz. The source is located 50 feet below the surface and sends out a 10 degree vertical beam at a grazing angle of 20 degrees. The receiver is also 50 feet below the surface and positioned in the line of the specular reflection.

Figure 5-2 shows the incident pulse and five reflected pulses calculated by using five different representations of a sea generated by a 10 knot wind. For the computer print-out the largest sample of each reflected wave was normalized to one. Compared to a total energy of 1.0 for the pulse reflected from

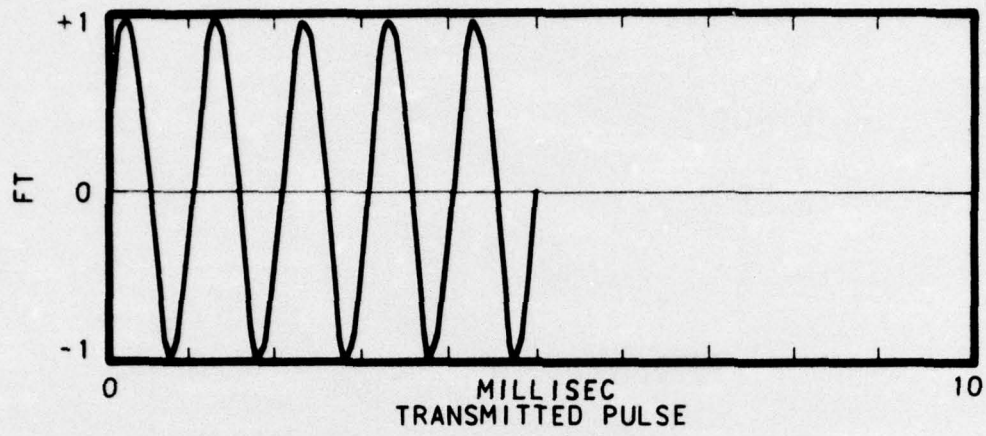

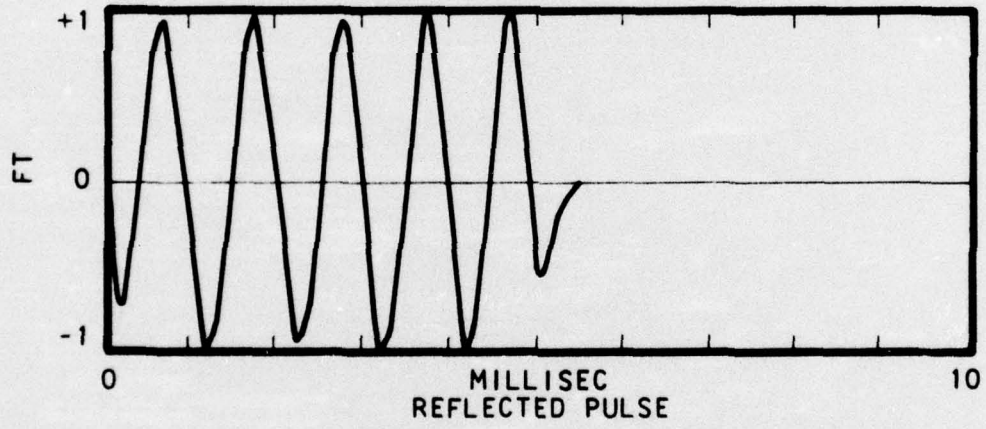

FIG. 5-1 TRANSMITTED AND REFLECTED PULSE FROM A FLAT OCEAN SURFACE

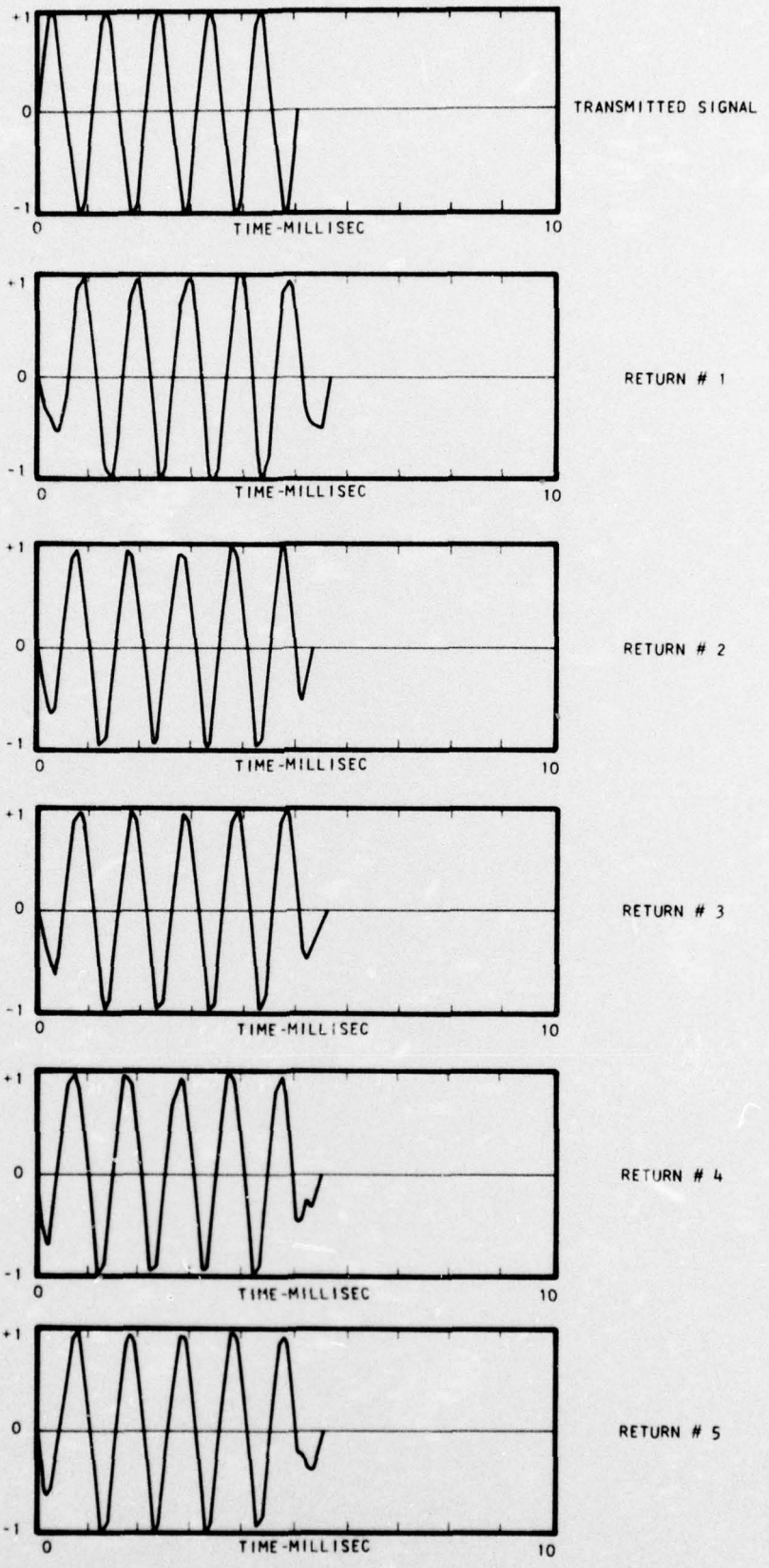

FIG. 5-2 - TRANSMITTED SIGNAL AND FIVE RETURNS FOR A 10 KNOT WIND GENERATED SURFACE

a flat surface the relative energies of the five reflected signals are 0.77, 0.99, 0.78, 0.79, and 0.55. In the next section the values are converted to dB levels with the mean and standard deviation listed in Table 6-1.

Figure 5-3 shows the incident and reflected pulses for a 20 knot wind speed. The relative energy ratios for the reflected waves are 0.29, 1.24, 0.13, 0.58, and 0.09.

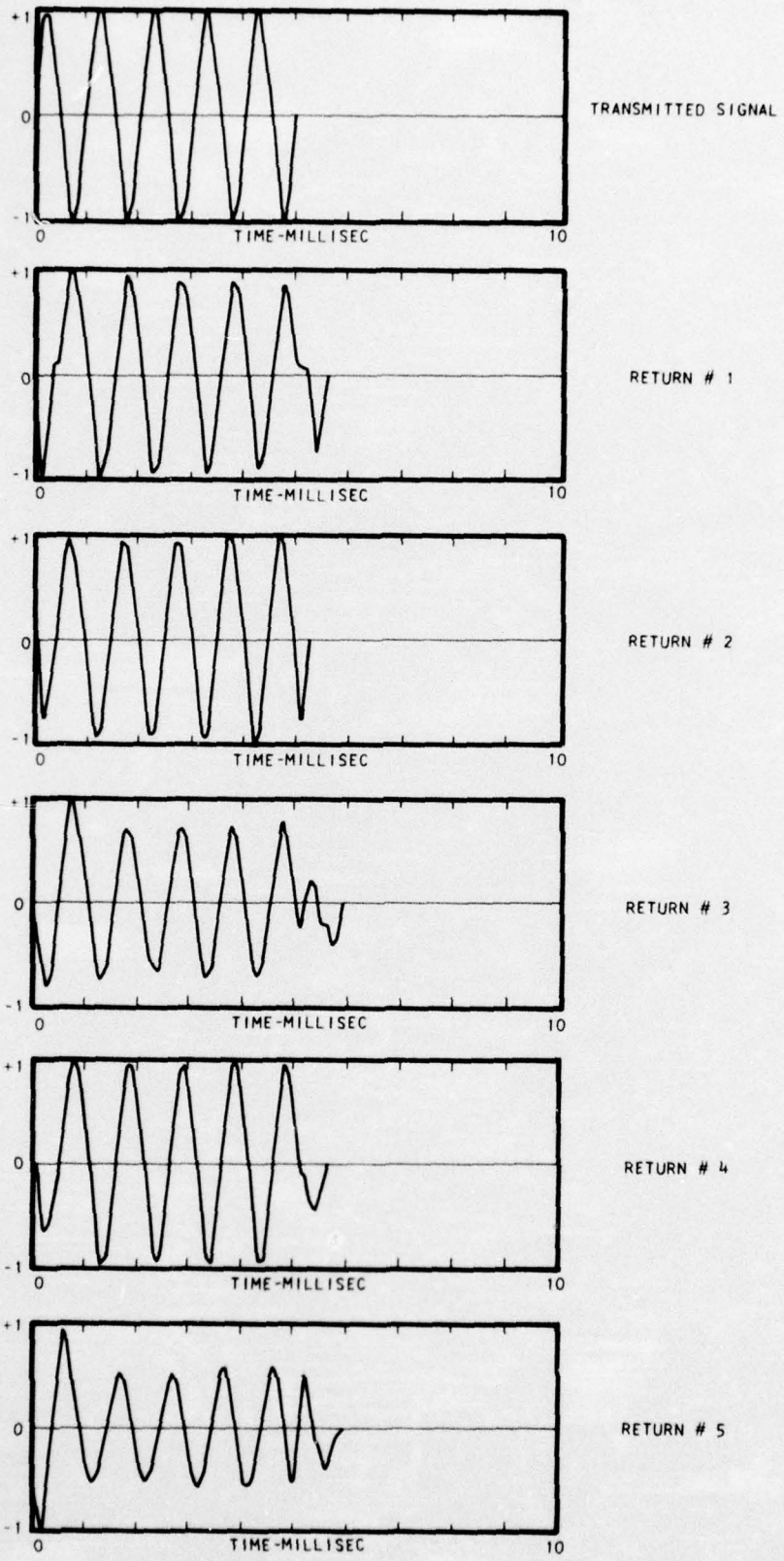

FIG. 5-3 -TRANSMITTED SIGNAL AND FIVE RETURNS FOR A 20 KNOT WIND GENERATED SURFACE

6. DISTORTION IN THE REFLECTED PULSE

After the reflected signal is calculated the question arises, by what criterion should be distortion be measured? Here, distortion is defined in terms of the loss of correlation that an optimum linear processor would suffer because of the distorted form of the reflected signal.

It is well known that the optimum linear processor for identifying a known signal in white noise (i.e., produces maximum S/N ratio at output) can be realized as a matched filter or as a linear replica correlator[23]. In the present work the Fast Fourier Transform method is used to calculate the correlation between the surface reflected signal and the incident signal.

Let $\{y_k, k = 0, 1, 2, \ldots, K-1\}$ represent K equally spaced samples of the signal reflected from the surface and $\{x_k, k = 0, 1, 2, \ldots K'-1\}$ represent samples from the incident signal. Since the reflected signal is extended in time by the reflection process, K is greater than K′. The correlation of the two signals, C_s, corresponding to a time lag sT, T = time interval between samples, is given by

$$C_s = \sum_{k=0}^{K-1-s} x_k \, y_{k+s} \quad . \tag{6.1}$$

For long pulses, the time required for evaluating Eq. (6.1) can be substantially reduced by using the Fast Fourier Transform. The details of the Fast Fourier method will be discussed next to prove that the correct answer is obtained and to illustrate the required arrangement of $\{x_k\}$ and $\{y_k\}$.

Let X_k be a sequence of 2N numbers, the first K′ of which are the same as x_k with the remaining terms set equal to zero. The value of N is specified by requiring that $N = 2^p$, where p is the smallest integer such that $2^p \geq K$. Let Y_k be

a sequence of 2N numbers, the first N of which are zero, the next K of which satisfy the relation $Y_{N+k} = y_k$, with the last remaining terms set equal to zero. Let A_r be components of the discrete Fourier transform (DFT) of $\{X_k\}$ and B_r be components of the DFT of $\{Y_k\}$. That is,

$$A_r = \sum_{k=0}^{2N-1} X_k \, W^{rk}$$

$$B_r = \sum_{\ell=0}^{2N-1} Y_\ell \, W^{r\ell}$$

where,

$$W \equiv \exp(-\pi i/N) \quad . \tag{6.2}$$

Next, form the sequence $\{D_r\}$ where D_r is the product of complex conjugate of A_r times B_r. The inverse discrete Fourier transform of $\{D_r\}$ can then be written as

$$\frac{1}{2N} \sum_{r=0}^{2N-1} A_r^+ \, B_r \, W^{-rs} = \frac{1}{2N} \sum_r \sum_k \sum_\ell X_k \, Y_\ell \, W^{-rk} \, W^{r\ell} \, W^{-rs}$$

$$= \frac{1}{2N} \sum_k \sum_\ell X_k \, Y_\ell \sum_r W^{r(\ell-k-s)}$$

$$= \sum_{k=0}^{2N-1-s} X_k \, Y_{k+s} + \sum_{k=2N-s}^{2N-1} X_k \, Y_{k+s-2N} \tag{6.3}$$

The last line follows from the fact that $\sum_{r=0}^{2N-1} W^{rn}$ equals 0 when n is an integer, except when n = 0, ±2N, ±4N, ... in which case

the sum is equal to 2N. The last sum is zero, because of the zeroes in $\{X_k\}$ and $\{Y_k\}$. The other sum in the last line is the desired correlation function C_s. The above arguments are similar to those used by Cochran et al.[24] in the evaluation of convolution integrals.

The auto-correlation function for the incident signal is shown at the top of Fig. 6-1 and the five cross-correlation functions for the reflected pulse at 10 knot wind speed are shown below. All of the correlograms are normalized to a peak value of one. The correlator output is squared and averaged over a 5 msec period in a detector. The detector outputs are shown in Fig. 6-2. The correlograms corresponding to a 20 knot wind speed are shown in Fig. 6-3. The detector outputs are similar in form to those in Fig. 6-2 and are not shown.

The effect of the surface reflection on processor performance is summarized in Table 6-1. First there is a performance loss because the energy level is down. This is shown in column 1 where the reference energy level is that of the signal reflected from the flat surface. The next column is the standard deviation of the energy levels divided by the five-sample mean energy level.

The total correlation loss is shown in column 5. This was calculated by comparing the average correlator output energy for the signal reflected from the time-varying surface to that for the signal reflected from the flat surface. The fluctuations in this correlation loss are given in column 6.

The total correlation loss can be separated into two parts. Part is due to the energy loss and part results from the distortion of the signal. The correlation loss due to distortion is the difference between the total loss and the energy loss. This is shown in column 3. As shown, the total loss for a 10 knot wind is 1.6 dB which is all due to energy loss. At 20 knot wind speed the total loss is 3.9 dB, 3.8 dB because of energy loss and 0.1 dB because of distortion.

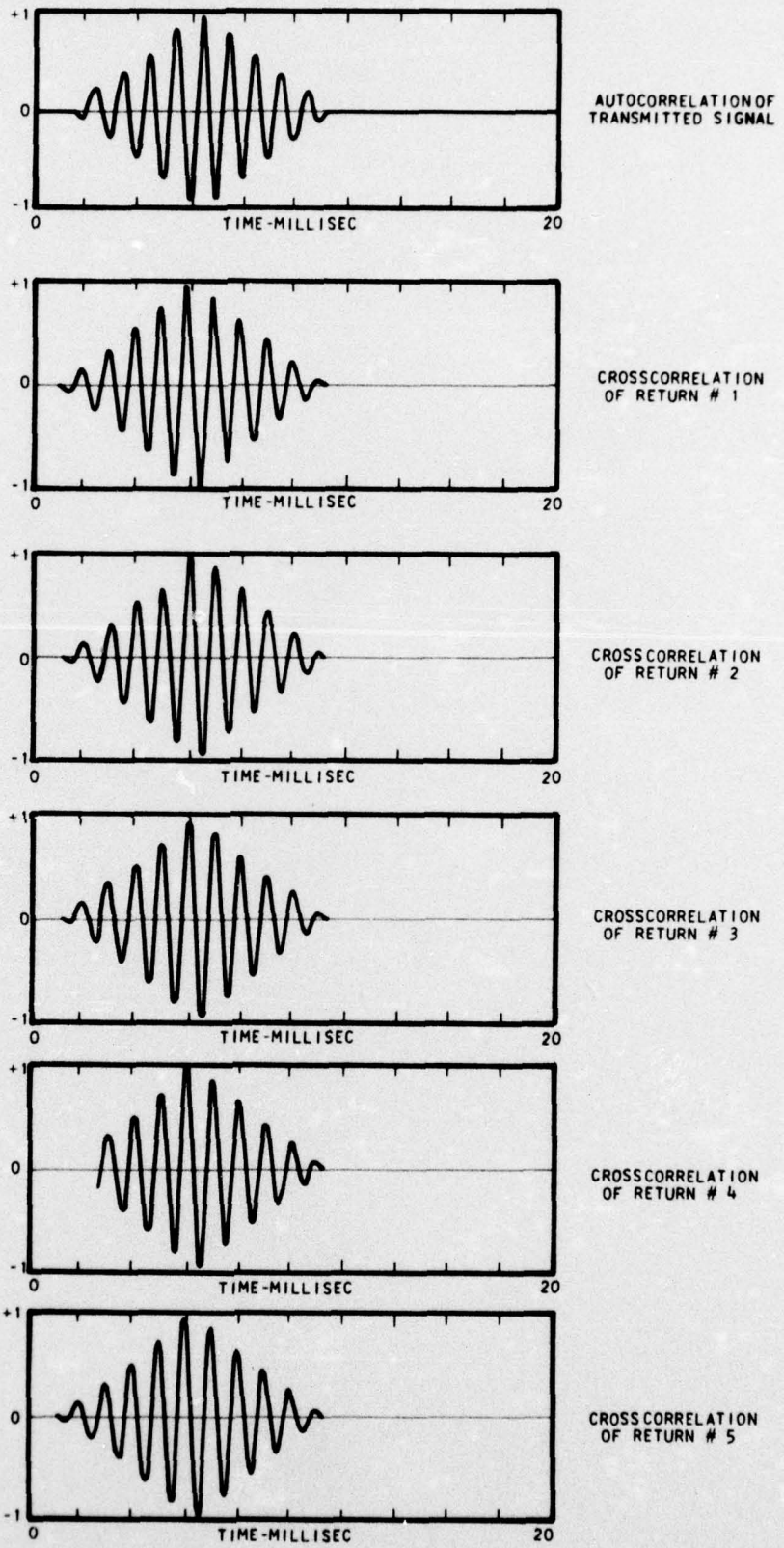

FIG. 6-1 - CROSSCORRELATION FUNCTIONS OF THE SIGNALS SHOWN IN FIG. 5.2 CORRELATED WITH THE TRANSMITTED SIGNAL (10 KNOT WIND SPEED)

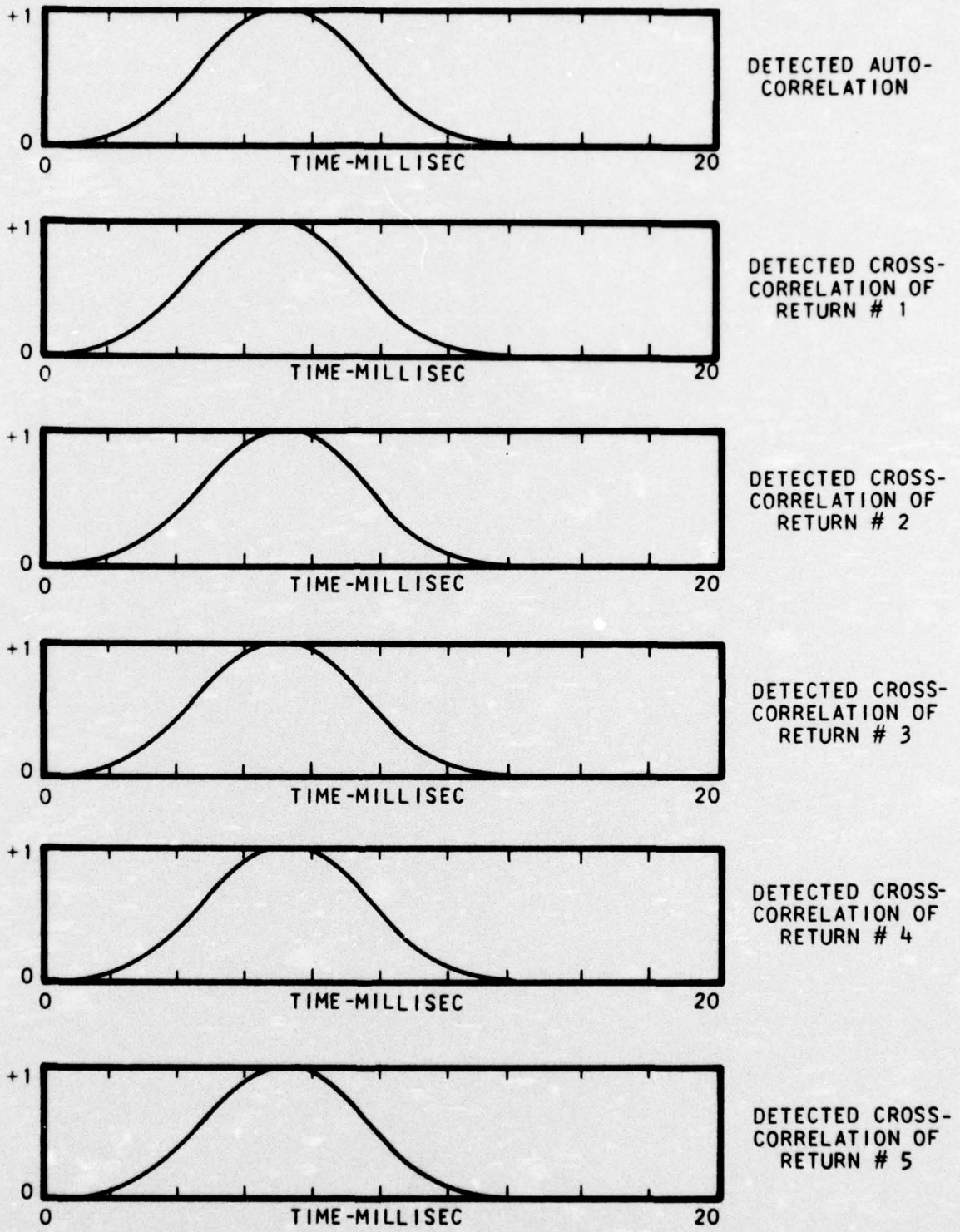

FIG. 6-2 - CROSSCORRELATION FUNCTIONS OF FIG. 6-1 AFTER SQUARE LAW RECTIFICATION AND PERFECT AVERAGING (10 KNOT WIND SPEED)

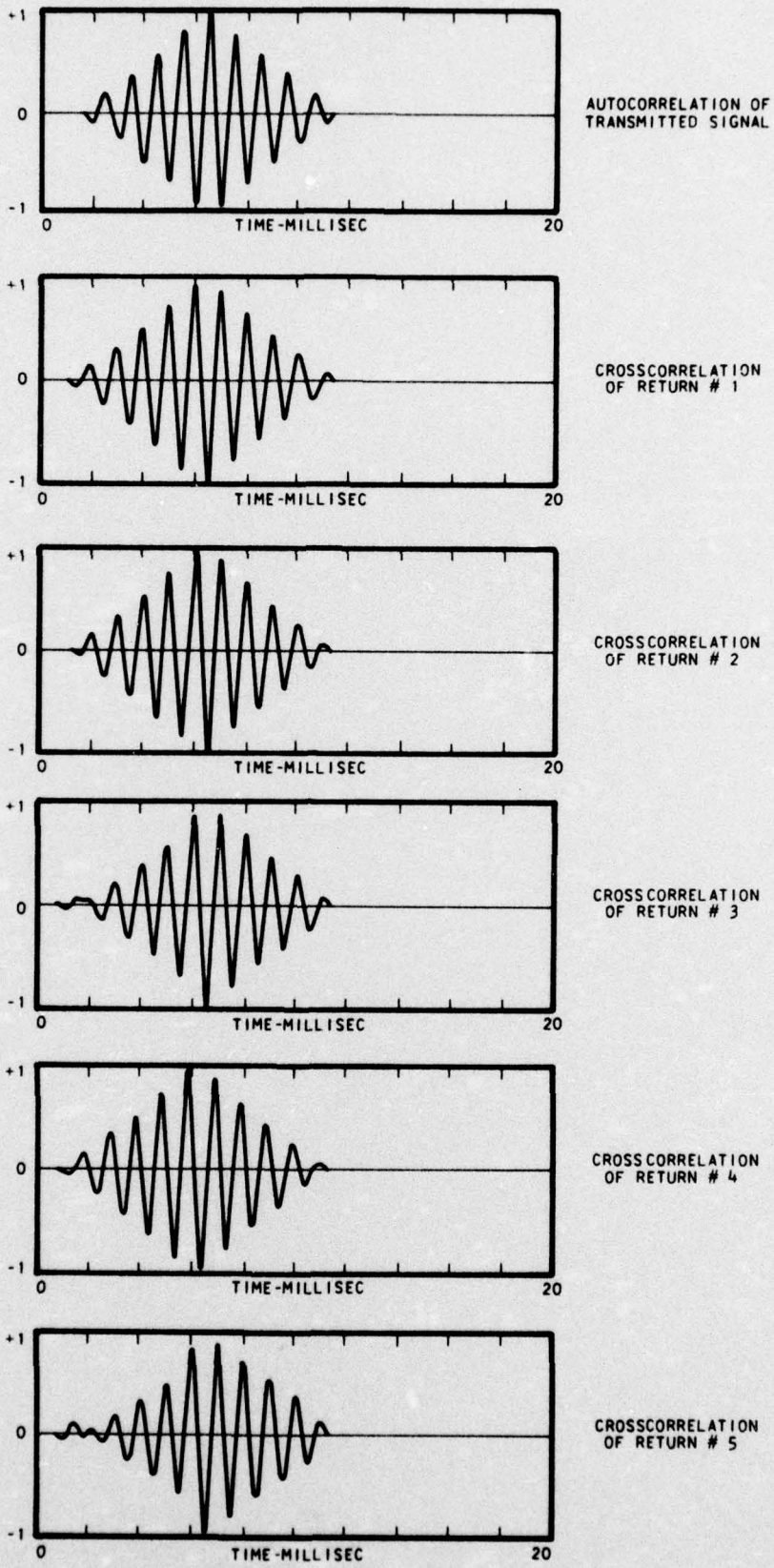

FIG. 6-3 - CROSSCORRELATION FUNCTIONS OF THE SIGNALS SHOWN IN FIG. 5-3 CORRELATED WITH THE TRANSMITTED SIGNAL (20 KNOT WIND SPEED)

	MEAN ENERGY LEVEL	STANDARD DEVIATION OF ENERGY DIVIDED BY MEAN	MEAN CORRELATION LOSS DUE TO SIGNAL DISTORTION	STANDARD DEVIATION OF DISTORTION CORRELATION LOSS DIVIDED BY MEAN	MEAN TOTAL CORRELATION LOSS	STANDARD DEVIATION OF TOTAL CORRELATION LOSS DIVIDED BY MEAN
FLAT SURFACE	0	0	0	0	0	0
10 KNOT SURFACE	-1.6 DB	.18	0.0 DB	.0058	1.6 DB	.178
20 KNOT SURFACE	-3.8 DB	.45	0.1 DB	.0982	3.9 DB	.296

TABLE 6-1 - EFFECTS OF SURFACE REFLECTION ON A 5 MILLISEC F.M. SLIDE PULSE

7. DISTORTED REPLICA CORRELATION

Because small improvements in the figure of merit of a sonar system will generally result in a large increase of the maximum detection range, great effort is spent to see that each part of the system operates with maximum efficiency. However, there are fundamental limits on each component. For example, the onset of cavitation restricts the maximum transducer radiation power while the physical size of the transducer limits the directivity factor of the beam. For the signal processing sections of the sonar system the theoretical limits of performance are not as well set.

In this report, the signal processing consists of correlation plus detection. The correlator multiplies the received signal $y(t)$ by a time shifted replica signal $r(t-\tau)$. Here τ is the time shift or time lag and $r(t)$ is generally set equal to the signal sent out, denoted $x(t)$. It is well known that this type of correlator, called the linear replica correlator, is the optimum (i.e., produces the largest signal-to-noise ratio) linear system if the returning signal, $y(t)$, has the form $y(t) = \text{const.} \cdot x(t) + \text{white noise}$. In this section a method is developed for adjusting the replica to fit the distortion of the returning signal, thus improving the correlator. Other possibilities for modifying the replica would include increasing the pulse length by adding new cycles or adding low frequency components which would alter the envelope of the pulse. In Fig. 7-1 are shown a sine cycle [$\sin(2\pi t/T)$], a cycle of the same energy with second harmonic distortion ($.9 \sin(2\pi t/T) + .436 \sin(4\pi t/T)$), and a cycle of the same energy with third harmonic distortion ($.9 \sin(2\pi t/T + .436 \sin(6\pi t/T)$). Consider a sonar pulse made up of a set of sine cycles of form $\sin(2\pi t/T_n)$. For example, for a Doppler invariant FM slide, $T_n = T_o + n \cdot \Delta T$, where T_o and ΔT are constants. If the returning signal is not exactly the same

as the signal sent out, a greater processor gain will be obtained using a replica made up of distorted cycles of form $[a_1 \sin(2\pi t/T_n) + a_2 \sin(4\pi t/T_n) + a_3 \sin(6\pi t/T_n)]$, $a_1^2 + a_2^2 + a_3^2 = 1$, than for a replica of the same as the outgoing pulse. The requirement $a_1^2 + a_2^2 + a_3^2 = 1$ will insure that, for a noise input, the rms level of the correlator output will not change as the replica is distorted. Let $c_1(\tau)$ be the result of correlating the return with the outgoing pulse, $c_2(\tau)$ be the result of correlating the return with a pulse made up of second harmonic cycles ($\sin 4\pi t/T_n$), and $c_3(\tau)$ the result of correlating with 3rd harmonic cycles. The correlation of the return with the distorted replica is then

$$C_D(\tau) = \sum_{i=1}^{3} a_i \, c_i(\tau) \; ; \; \sum_{i=1}^{3} a_i^{\,2} = 1 \; . \qquad (7.1)$$

The problem is to maximize $C_D(\tau)$ by proper choice of a_1, a_2 and a_3. A maximum value of $C_D(\tau)$ corresponds to a maximum value of $C_D^{\,2}(\tau)$. Further, it is noted that since $C_D(\tau)$ and $C_D^{\,2}(\tau)$ have a rapid fluctuation as τ changes it would be of more significance to choose the a's to maximize $\overline{C_D^{\,2}(\tau)}$ where the bar denotes a time average. In this case $\overline{C_D^{\,2}(\tau)}$ corresponds to the output of a processor that consists of a linear distorted replica correlator followed by a square law detector and a perfect averager. Let τ_o be the time lag that the processor has maximum output when correlating the output with the input, i.e.,

$$\frac{\text{time}}{c_1^{\,2}(\tau_o)} = \text{max.} \qquad (7.2)$$

The problem is then to choose a_1, a_2 and a_3 such that $\overline{C_D^{\,2}(\tau_o)} =$ max. Using the method of Lagrangian multipliers results in three equations.

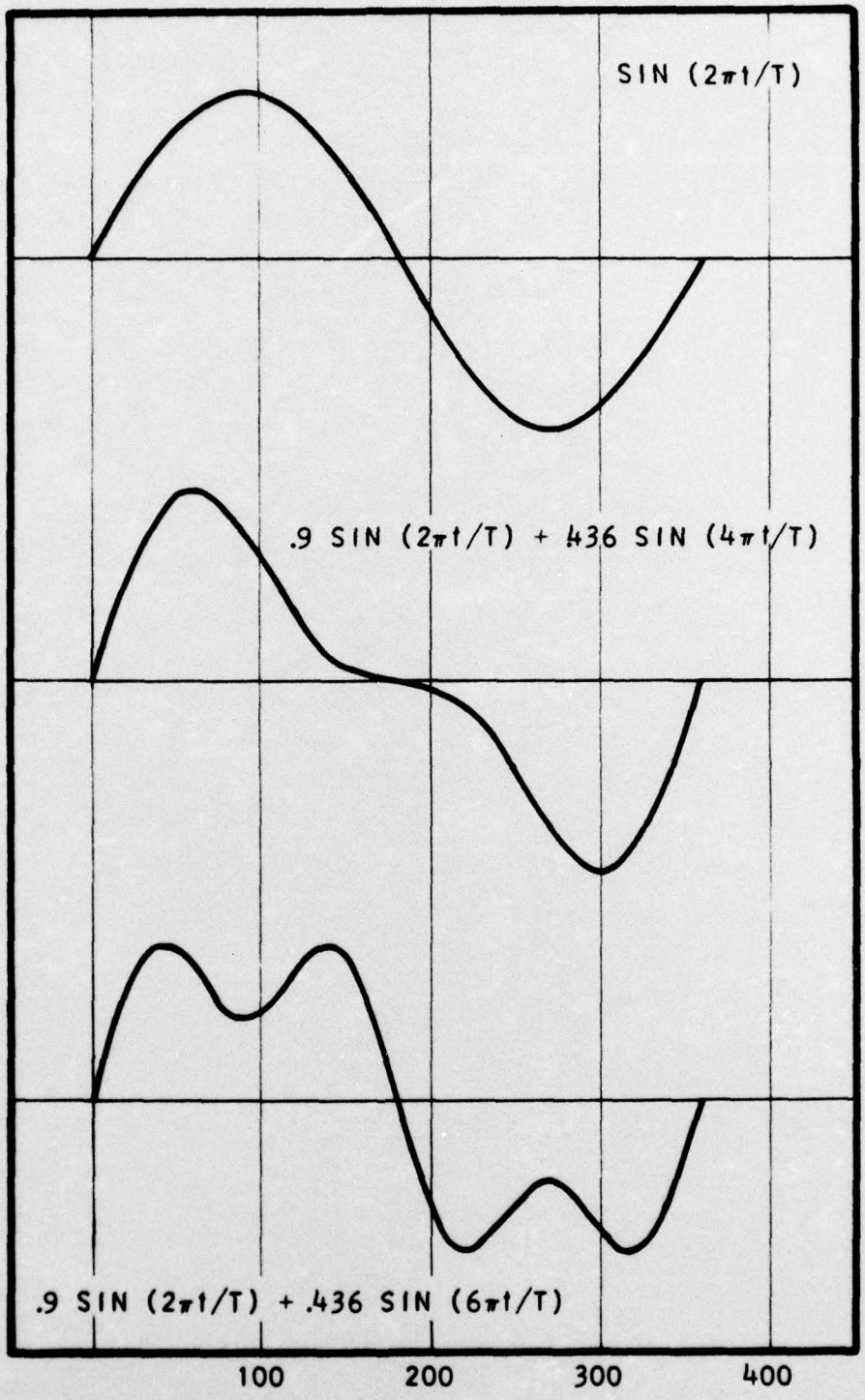

FIG. 7-1 - DISTORTED REPLICAS

$$a_1(\overline{C_1^2} - \lambda) + a_2\,\overline{C_1C_2} + a_3\,\overline{C_1C_3} = 0$$

$$a_2\,\overline{C_1C_2} + a_2(\overline{C_2^2} - \lambda) + a_3\,\overline{C_2C_3} = 0$$

$$a_3\,\overline{C_1C_3} + a_2\,\overline{C_2C_3} + a_3(\overline{C_3^2} - \lambda) = 0 \quad . \qquad (7.3)$$

Here λ is the Lagrangian multiplier, which can be shown to equal $\overline{C_D^2}$,($\lambda = \overline{C}_D^2$). The above Eq. (7.3) has the trivial solution, $a_1 = a_2 = a_3 = 0$, unless the determinant of the coefficients of the a's is identically zero. Solution of this determinant leads to three values of λ, the largest of which corresponds to the maximum correlator output. Substituting this value of λ back into any two of the equations in (7.3) results in values of the ratios a_2/a_1 and a_3/a_1. Now requiring that $a_1^2 + a_2^2 + a_3^2 = 1$ completes the solution

The utility of this type of processing depends upon the amount of improvement and whether or not the coefficients a_2 and a_3 measured in a large number of cases have mean values significantly different from zero. For example, if for 1000 experimental pulses maximum correlation was obtained for a set of a_2's with mean 0.01 and standard deviation 0.1, it would not be worthwhile to correct for second order distortion since in almost half of the cases setting $a_2 = 0.01$ would reduce the processor output. However, if the mean was 0.1 and the standard deviation was 0.01, then the use of this correction would depend, among other factors, upon whether or not the processing gain was significant.

Distorted replica correlation was tried on 7 samples of the 5 msec pulse described in Section 5. The mean value of a_2 was calculated to be .004 with a standard deviation equal to .0003. The mean value of a_3 was -.006 with a standard deviation equal to .001. The mean processing gain for the "best" replica in each case was only .003 dB. Because these calculations are expensive, in terms of computer time, and because of the negligible gain in processor output, no further cases were run.

Although the result of this effort was negative the result has significance. Modifying the shape of the replica in a significant manner had essentially no effect on the processor output. Thus, at least for the pulse forms and ocean surfaces tested here, there was no significant processing gain obtainable by matching the return to a replica with second and third order harmonic distortion.

8. IRREGULAR SIGNAL FORMS

In preceding sections sonar pulses have been formed by stringing together a set of sine cycles. This is an excellent representation of CW or FM pulses but fails to represent the pseudo-random noise pulse or an explosive pulse. In these cases a generalization of the preceding theory can be used.

Consider the set f_1, f_2, f_3, ... obtained by sampling the signal f at times t_1, t_2, t_3, ... where $t_n = n\Delta t$. If Δt is chosen such that the sampling rate is twice the highest significant frequency component in f then, by Shannon's sampling theorem, f is completely described by f_1, f_2, f_3, ... The next step will be to fill in between the f_i with a well behaved function that is amenable to integration by use of Kirchoff's integral. Consider the points f_1, f_2 and f_3 shown as ■'s in Fig. 8-1. A smooth curve of form $A_1 \sin(2\pi t/T_1 + \varphi_1) + B_1$ is fit between these points. A second curve of the same form, $A_2 \sin(2\pi t/T_2 + \varphi_2) + B_2$, is fit between f_3, f_4, and f_5 with the restriction that it match the slope of curve at f_3. This requires solution of a set of four transcendental equations for the four constants a_2, T_2, φ_2 and b_2. It may be that the solution of the transcendental equations can only be made in the least mean square error sense. If the least error is not acceptable the requirement that the curve pass through f_5 can be dropped with the next new curve beginning at f_4 rather than f_5.

The form of the above curves is well suited for use with material developed in earlier sections since for each piece of the curve [f] and [f'] have simple forms. Thus the evaluation of Eq. (4.6) is not much more complicated than it is for f(t) made up of a set of complete sine cycles.

Other mathematical forms can be used to represent f(t), for example, straight line segments. Combinations of forms are possible such as an explosive pulse represented by a linear

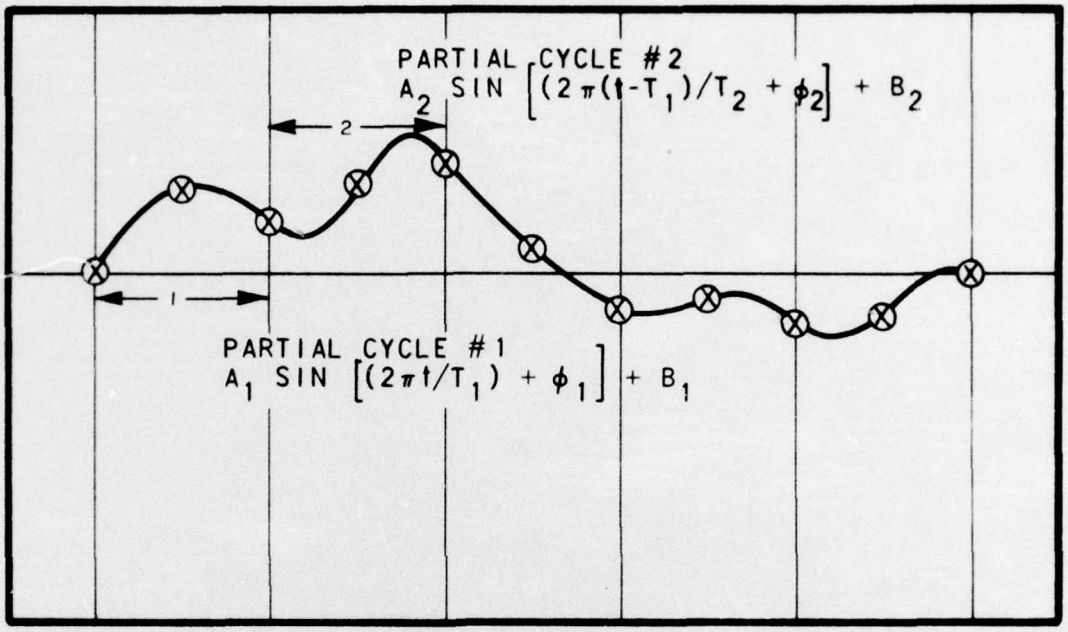

FIG. 8-1 - IRREGULAR SIGNAL FORM

pressure rise with an exponential function for the fall off. Two restrictions must be kept in mind, however. First, f(t) must be continuous. Otherwise, there will be a delta function contribution from the [f′] term in Eq. (4.6). Second, when the time duration of a section of f(t) is decreased there may be a corresponding reduction in the maximum size of surface elements, since any element must be smaller than the region covered by any segment of f(t) reflecting from the surface.

9. CONCLUSIONS

This report covers the first phase of a research project to study the correlation loss of a sonar pulse when it reflects from the time-varying ocean surface. A method for calculating the reflected pulse has been developed, based on Kirchoff's integral, and a computer program has been written to do the computations. Test runs on a short pulse (5 msec) show an average correlation loss of 1.6 dB for a pulse reflecting from the sea driven by a 10 knot wind, and 3.9 dB for a pulse reflected from a 20 knot sea. Almost all of the correlation loss is due to an energy loss in the reflected pulse.

The next phase of this work will concern the correlation loss of longer pulses. Other interesting and useful problems include the study of reflection of wide beams, the correlation loss of pseudo-random noise signals, the addition of capillary waves and white caps to the sea surface, non-specular scattering, and so on. All of these problems can be studied with little or no modification of the basic theory developed here.

Some preliminary calculations for 100 msec FM slides at 1 kHz and 3.5 kHz have been run. These tend to show slightly smaller energy and correlation losses than for the short test pulses.

REFERENCES

1. R. J. Urick and R. M. Hoover, "Backscattering of Sound from the Sea Surface: Its Measurement, Causes, and Application to the Prediction of Reverberation Levels," J. Acoust. Soc. Amer. 28, 1038-1042 (1956).

2. G. R. Garrison, S. R. Murphy, and D. S. Potter, "Measurement of the Backscattering of Underwater Sound from the Sea Surface," J. Acoust. Soc. Amer. 32, 104-111 (1960).

3. R. P. Chapman and J. H. Harris, "Surface Backscattering Strength Measured with Explosive Sound Sources," J. Acoust. Soc. Amer. 34, 1592-1597 (1962).

4. H. W. Marsh, "Sound Reflection and Scattering from the Sea Surface," J. Acoust. Soc. Amer. 35, 240-244 (1963).

5. R. M. Richter, "Measurements of Backscattering from the Sea Surface," J. Acoust. Soc. Amer. 36, 864-869 (1964).

6. L. N. Liebermann, "Reflection of Underwater Sound from the Sea Surface," J. Acoust. Soc. Amer. 20, 498-503 (1948).

7. L. M. Brekhovskikh, "Diffraction of Waves on a Rough Surface: General Theory and Applications," J. Exper. and Theoretical Physics (in Russian), 23, 275-304 (1952).

8. Carl Eckart, "The Scattering of Sound from the Sea Surface," J. Acoust. Soc. Amer. 25, 566-570 (1953).

9. W. C. Meecham, "Fourier Transform Method for the Treatment of the Problem of Radiation from Irregular Surfaces," J. Acoust. Soc. Amer. 28, 370-377 (1956).

10. H. W. Marsh, "Exact Solution of Wave Scattering by Irregular Surfaces," J. Acoust. Soc. Amer. 33, 330-333 (1961).

11. J. L. Uretsky, "The Scattering of Plane Waves from Periodic Surfaces," Annals of Physics, 33, 400-427 (1965).

12. B. E. Parkins, "Omnidirectional Scattering of Acoustic Waves by Rough, Imperfectly Scattering Surfaces," J. Acoust, Soc. Amer. 41, 126-134 (1967).

13. E. O. La Casce and P. Tamarkin, "Underwater Sound Reflection from a Corrugated Surface," J. Acoust. Soc. Amer. 27, 138-148 (1956).

14. C. W. Horton, S. K. Mitchell, and G. R. Barnard, "Model Studies on the Scattering of Waves from a Rough Surface," J. Acoust. Soc. Amer. 41, 635-643 (1967).

15. Herman Medwin, "Specular Scattering of Underwater Sound from a Wind-Driven Surface," J. Acoust. Soc. Amer. 41, 1485-1495 (1967).

16. L. N. Leibermann, "Analysis of Rough Surfaces by Scattering," J. Acoust. Soc. Amer. 35, 932 (1963).

17. H. W. Marsh, "Doppler of Boundary Reverberation," J. Acoust. Soc. Amer. 35, 1836 (1963).

18. B. E. Parkins, "Scattering from the Time-Varying Surface of the Ocean," J. Acoust. Soc. Amer. 42, 1262-1267 (1967).

19. G. Neumann and W. J. Pearson Jr., Principles of Physical Oceanography (Prentice-Hall, Inc., Englewood Cliffs, N. J., 1966), Chap. 12, pp. 336-351.

20. W. J. Pearson Jr. and L. Moskowitz, "A Proposed Spectral Form for Fully Developed Wind Seas Based on the Similarity Theory of S. A. Kitaigorodskii," J. Geophys. Res. 69, 5181-5190 (1964).

21. B. B. Baker and E. T. Copson, The Mathematical Theory of Huygens Principle (Oxford University Press, London, 1939), pp. 36-45.

22. R. J. Wagner, "Shadowing of Randomly Rough Surfaces," J. Acoust. Soc. Amer. 41, 138-147 (1967).

23. L. A. Zadeh and J. R. Ragazzini, "Optimum Filters for the Detection of Signals in Noise," Proc. IRE, 40 (10), 1123-1131 (1952).

24. W. T. Cochran et.al (the G-AE Subcommittee on Measurement Concepts), "What is the Fast Fourier Transform?", IEEE Trans., Vol. AU-15, No. 2, (1967).

Unclassified
Security Classification

DOCUMENT CONTROL DATA - R&D

(Security classification of title, body of abstract and indexing annotation must be entered when the overall report is classified)

1 ORIGINATING ACTIVITY (Corporate author)
TRACOR, Inc.

2a REPORT SECURITY CLASSIFICATION
Unclassified

2b GROUP

3 REPORT TITLE
"THE DISTORTION OF A SONAR PULSE REFLECTED FROM THE OCEAN SURFACE"

4 DESCRIPTIVE NOTES *(Type of report and inclusive dates)*
Technical Memorandum

5 AUTHOR(S) *(Last name, first name, initial)*
Bucker, H. P. and Bourianoff, G. I.

6 REPORT DATE
March 1, 1968

7a TOTAL NO. OF PAGES
44

7b NO. OF REFS
24

8a CONTRACT OR GRANT NO.
N00024-67-C-1318

b PROJECT NO.
SF101-03-16

Task 8524

9a ORIGINATOR'S REPORT NUMBER(S)
68-343-U

9b OTHER REPORT NO(S) *(Any other numbers that may be assigned this report)*

10 AVAILABILITY/LIMITATION NOTICES

11 SUPPLEMENTARY NOTES

12 SPONSORING MILITARY ACTIVITY
Naval Ship Systems Command
Department of the Navy
Washington, D. C. 20360

13 ABSTRACT

Equations are derived for the direct evaluation of a sonar pulse reflected from a time-varying ocean surface. Fewer assumptions and approximations are made in this direct approach than in conventional developments of scattering theory. However, the cost of computer time may become excessive for some cases.

The calculated surface reflected signals are correlated with the incident sonar pulse to find the expected correlation loss of a sonar processor. For a short (5 msec) low frequency FM slide the calculated correlation losses (1.6 dB for the surface generated by a 10 knot wind and 3.9 dB for a 20 knot wind) were almost entirely the result of energy loss in the reflected signal.

DD FORM 1 JAN 64 1473

Unclassified
Security Classification

14 KEY WORDS	LINK A		LINK B		LINK C	
	ROLE	WT	ROLE	WT	ROLE	WT

INSTRUCTIONS

1. ORIGINATING ACTIVITY: Enter the name and address of the contractor, subcontractor, grantee, Department of Defense activity or other organization *(corporate author)* issuing the report.

2a. REPORT SECURITY CLASSIFICATION: Enter the overall security classification of the report. Indicate whether "Restricted Data" is included. Marking is to be in accordance with appropriate security regulations.

2b. GROUP: Automatic downgrading is specified in DoD Directive 5200.10 and Armed Forces Industrial Manual. Enter the group number. Also, when applicable, show that optional markings have been used for Group 3 and Group 4 as authorized.

3. REPORT TITLE: Enter the complete report title in all capital letters. Titles in all cases should be unclassified. If a meaningful title cannot be selected without classification, show title classification in all capitals in parenthesis immediately following the title.

4. DESCRIPTIVE NOTES: If appropriate, enter the type of report, e.g., interim, progress, summary, annual, or final. Give the inclusive dates when a specific reporting period is covered.

5. AUTHOR(S): Enter the name(s) of author(s) as shown on or in the report. Enter last name, first name, middle initial. If military, show rank and branch of service. The name of the principal author is an absolute minimum requirement.

6. REPORT DATE: Enter the date of the report as day, month, year, or month, year. If more than one date appears on the report, use date of publication.

7a. TOTAL NUMBER OF PAGES: The total page count should follow normal pagination procedures, i.e., enter the number of pages containing information.

7b. NUMBER OF REFERENCES: Enter the total number of references cited in the report.

8a. CONTRACT OR GRANT NUMBER: If appropriate, enter the applicable number of the contract or grant under which the report was written.

8b, 8c, & 8d. PROJECT NUMBER: Enter the appropriate military department identification, such as project number, subproject number, system numbers, task number, etc.

9a. ORIGINATOR'S REPORT NUMBER(S): Enter the official report number by which the document will be identified and controlled by the originating activity. This number must be unique to this report.

9b. OTHER REPORT NUMBER(S): If the report has been assigned any other report numbers *(either by the originator or by the sponsor)*, also enter this number(s).

10. AVAILABILITY/LIMITATION NOTICES: Enter any limitations on further dissemination of the report, other than those imposed by security classification, using standard statements such as:

(1) "Qualified requesters may obtain copies of this report from DDC."

(2) "Foreign announcement and dissemination of this report by DDC is not authorized."

(3) "U. S. Government agencies may obtain copies of this report directly from DDC. Other qualified DDC users shall request through _____."

(4) "U. S. military agencies may obtain copies of this report directly from DDC. Other qualified users shall request through _____."

(5) "All distribution of this report is controlled. Qualified DDC users shall request through _____."

If the report has been furnished to the Office of Technical Services, Department of Commerce, for sale to the public, indicate this fact and enter the price, if known.

11. SUPPLEMENTARY NOTES: Use for additional explanatory notes.

12. SPONSORING MILITARY ACTIVITY: Enter the name of the departmental project office or laboratory sponsoring *(paying for)* the research and development. Include address.

13. ABSTRACT: Enter an abstract giving a brief and factual summary of the document indicative of the report, even though it may also appear elsewhere in the body of the technical report. If additional space is required, a continuation sheet shall be attached.

It is highly desirable that the abstract of classified reports be unclassified. Each paragraph of the abstract shall end with an indication of the military security classification of the information in the paragraph, represented as *(TS)*, *(S)*, *(C)*, or *(U)*.

There is no limitation on the length of the abstract. However, the suggested length is from 150 to 225 words.

14. KEY WORDS: Key words are technically meaningful terms or short phrases that characterize a report and may be used as index entries for cataloging the report. Key words must be selected so that no security classification is required. Identifiers, such as equipment model designation, trade name, military project code name, geographic location, may be used as key words but will be followed by an indication of technical context. The assignment of links, rules, and weights is optional.